

# Manifold Learning for Hyperspectral Images

**Fethi Harkat**, Guillaume Gey, Valérie Perrier, Kévin Polisano,  
Tiphaine Debeuret

Université Grenoble Alpes

Whispers 2025



## 1 Introduction

- XRT Hyperspectral Data and Acquisition Process
- Objectives
- Motivation and Problem Statement

## 2 Methodology

- Proposed Pipeline
- UMAP for HSI

## 3 Experiments

- Segmentation for Cigarettes Dataset
- Regression for Stones Dataset
- Classification for Indian Pines Dataset

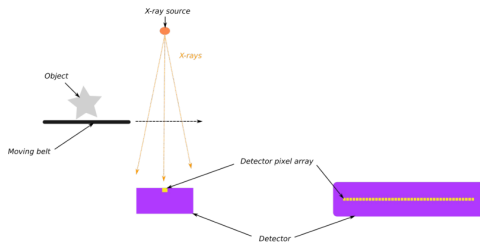
# XRT images

- **X-ray Transmission (XRT)** is a non-destructive imaging technique that measures how X-rays pass through an object.
- Used in **security screening**, **medical imaging**, and **industrial inspection**.
- Each material attenuates X-rays differently providing rich information about internal composition.



# XRT Hyperspectral Data and Acquisition Process

- The acquisition setup consists of:
  - A fixed X-ray source and a static detector array of 512 pixels.
  - A moving belt carrying the inspected object between them.
  - Continuous acquisition during object motion.
- This configuration allows capturing transmitted X-rays across multiple energy bands.



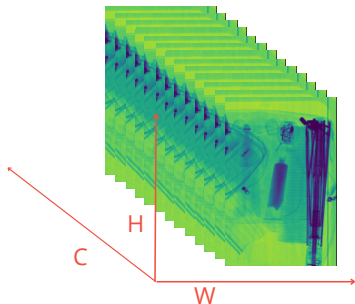
Side view of acquisition system

Top view of a detector

Experimental setup: X-ray source, moving belt, and static detector array.

# XRT Hyperspectral Data and Acquisition Process

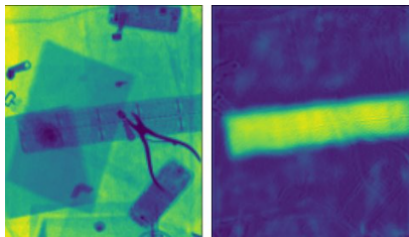
- The detector captures a sequence of X-ray transmission spectra over time.
- Each acquisition produces a 3D hyperspectral volume representing spatial–spectral information.



Example of an X-ray hyperspectral image:  $H$  and  $W$  are spatial dimensions,  $C$  is the spectral dimension.

# Objectives

- 1 Build expressive spectral representations.
- 2 Reduce dimensionality.
- 3 Evaluate the impact using deep learning models.



Cigarette Segmentation Example

# Motivation and Problem Statement

- Traditional techniques (PCA, NMF) fail to capture non-linear spectral correlations in XRT data.
- Hyperspectral XRT images exhibit high noise and complex variability.
- Such limitations lead to reduced CNN performance in decision-making tasks.

## 1 Introduction

- XRT Hyperspectral Data and Acquisition Process
- Objectives
- Motivation and Problem Statement

## 2 Methodology

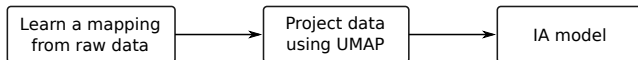
- Proposed Pipeline
- UMAP for HSI

## 3 Experiments

- Segmentation for Cigarettes Dataset
- Regression for Stones Dataset
- Classification for Indian Pines Dataset

# Proposed Pipeline

- 1 Train UMAP on raw data  $[H, W, C]$  to learn intrinsic structure.
- 2 Project to low-dimensional embedding  $[H, W, D]$ .
- 3 Feed the projection into CNN models for segmentation or regression.

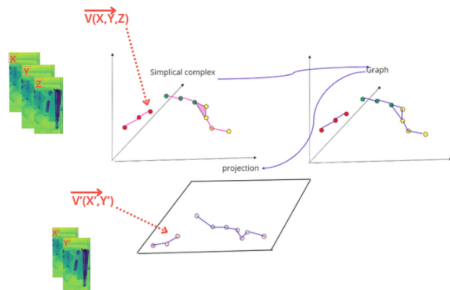


Pipeline: learning expressive low-dimensional features from XRT HSI.

# Introduction to UMAP

- **UMAP** (Uniform Manifold Approximation and Projection)<sup>1</sup> reduces data dimensionality using a **graph-based manifold learning** approach.
- Main idea:
  - 1 Build a simplicial complex from data.
  - 2 Convert it into a weighted graph.
  - 3 Optimize a low-dimensional projection that preserves topology.

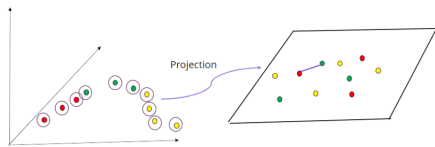
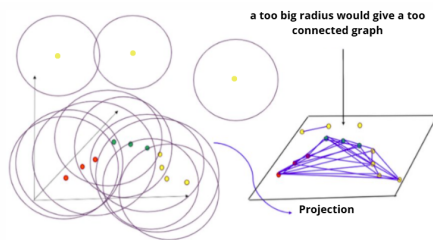
Open balls	Simplex	Nodes
	0 simplex (two points)	Nodes (two points)
	1 simplex (line segment)	Nodes (two points connected by an edge)
	2 simplex (triangle)	Nodes (three points forming a triangle)
	3 simplex (tetrahedron)	Nodes (four points forming a tetrahedron)



<sup>1</sup>McInnes, Healy, and Melville 2020.

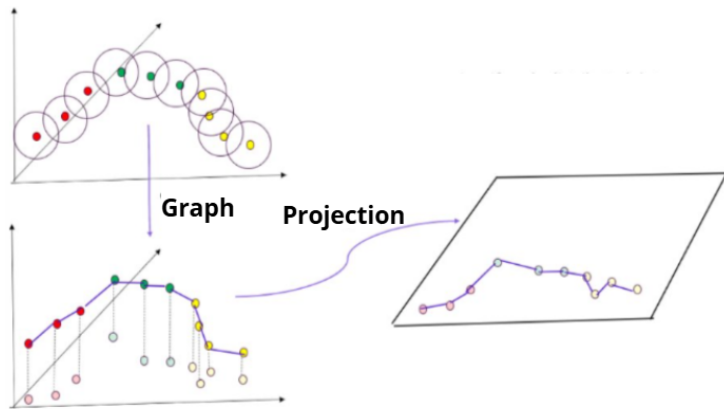
# Density Regions

After the graph creation which is depending on the chosen distance parameter (represented by the radius of a ball), two issues may arise:



**High- and low-density regions in the data space.**

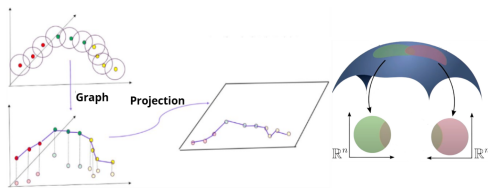
# What if it were uniformly distributed?



- Uniformity assumption: needed so that we can treat density uniformly and interpret distances meaningfully in the high-dimensional space.

# Uniform Manifold Approximation and Projection (UMAP)

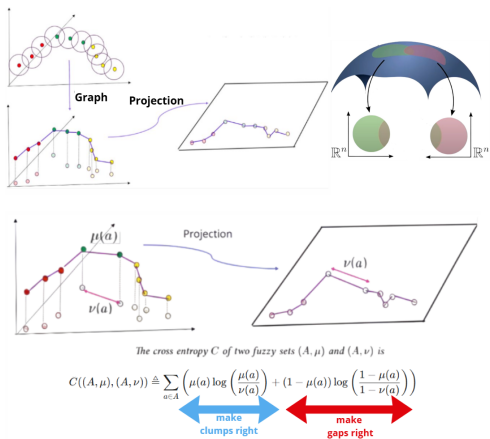
- Data are assumed to lie on a low-dimensional **Riemannian manifold** embedded in a higher-dimensional space.



What if it were uniformly distributed?

# Uniform Manifold Approximation and Projection (UMAP)

- Data are assumed to lie on a low-dimensional **Riemannian manifold** embedded in a higher-dimensional space.
- The embedding is learned by **optimizing a cross-entropy objective** that preserves pairwise similarities between data points.



## 1 Introduction

- XRT Hyperspectral Data and Acquisition Process
- Objectives
- Motivation and Problem Statement

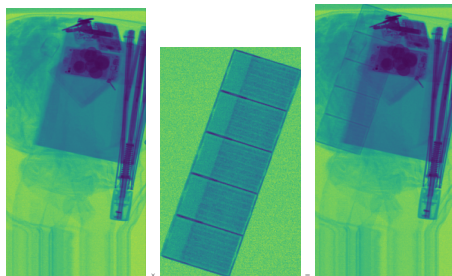
## 2 Methodology

- Proposed Pipeline
- UMAP for HSI

## 3 Experiments

- Segmentation for Cigarettes Dataset
- Regression for Stones Dataset
- Classification for Indian Pines Dataset

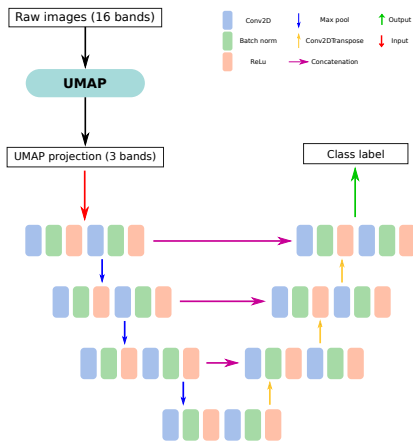
- **Cigarettes Dataset:** Synthetic and real luggage images for segmentation.



- **Stones Dataset:** Industrial samples for chemical composition and mass regression.
- **Indian Pines Dataset:** Benchmark HSI dataset for land-cover classification.

# Experiment 1: Cigarettes Dataset

- Task: binary segmentation (detect cigarettes in luggage).
- Dataset: 320 synthetic train, 30 synthetic test, 21 real test images.
- **CNN model:** U-Net.



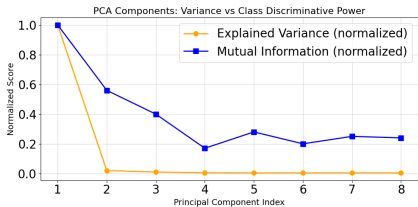
# Results – Cigarettes Dataset

Dataset	Method	Bands	Mean IoU	IoU Err	Mean Dice	Dice Err
Synthetic	Raw Data	16	0.766	0.032	0.865	0.005
	NMF	5	0.214	0.012	0.330	0.009
	PCA	5	0.417	0.012	0.572	0.005
	PCA	8	0.433	0.010	0.598	0.007
	<b>UMAP</b>	<b>5</b>	<b>0.833</b>	<b>0.016</b>	<b>0.901</b>	<b>0.006</b>
Real	Raw Data	16	0.230	0.020	0.370	0.010
	NMF	5	0.200	0.030	0.330	0.010
	PCA	5	0.180	0.030	0.300	0.010
	<b>UMAP</b>	<b>5</b>	<b>0.320</b>	<b>0.040</b>	<b>0.490</b>	<b>0.010</b>

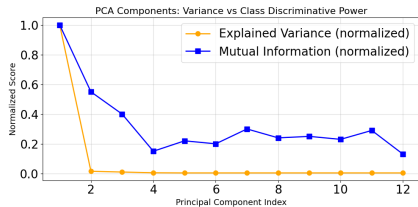
Comparison of segmentation performance across synthetic and real datasets for different dimensionality reduction methods.

- Outperforms PCA and NMF on both synthetic and real data.

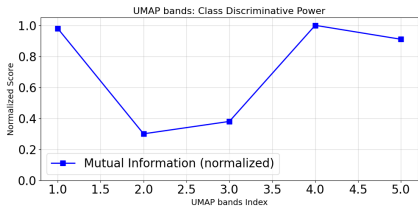
# Mutual Information Analysis



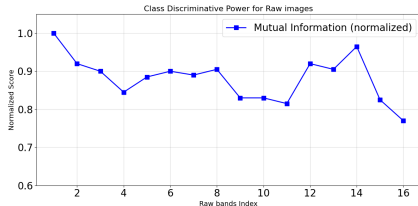
(a) PCA with 8 components



(b) PCA with 12 components



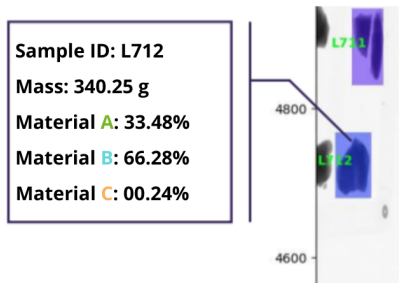
(c) UMAP with 5 bands



(d) Raw data with 16 bands

## Experiment 2: Stones Dataset

- Task: predict mass and material concentrations A, B.
- Dataset: 1453 train / 514 test images.



Stones data

- **CNN model:** 4 Inception blocks with regression head.

## SH-Score Definition

$$\text{SH} = M \frac{\prod_{i=1}^M S_i}{\sum_{i=1}^M S_i}, \quad S_i = \exp\left(-\frac{\sum_{j=1}^N |p_{ij} - t_{ij}|}{\sum_{j=1}^N t_{ij}}\right)$$

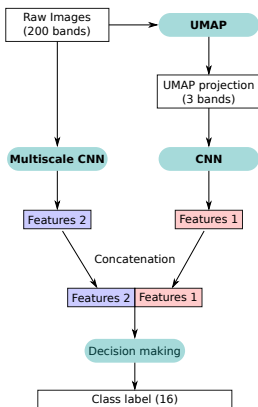
where  $M$  is the number of targets, and  $S_i \in [0, 1]$  the individual score.

Method	Bands	Mean SH	Err SH	Mean $S_A$	Err $S_A$	Mean $S_B$	Err $S_B$
RAW	64	0.598	0.008	0.528	0.006	0.964	0.003
NMF	20	0.596	0.006	0.512	0.011	0.963	0.004
PCA	20	0.617	0.005	0.538	0.006	0.964	0.003
UMAP	10	0.641	0.007	0.559	0.008	0.972	0.002
UMAP	20	<b>0.677</b>	0.003	<b>0.614</b>	0.008	<b>0.974</b>	0.002
UMAP	30	0.636	0.006	0.552	0.005	0.970	0.001

- 20-band UMAP achieves optimal balance of compression and accuracy.
- UMAP-based representations outperform PCA and NMF.

# Experiment 3: Indian Pines Dataset

- AVIRIS dataset:  $145 \times 145$  pixels, 220 spectral bands, 16 land-cover classes.
- **CNN model:** Multiscale CNN with two parallel input branches:
  - Raw hyperspectral image.
  - 3-band UMAP projection.



# Results – Indian Pines Dataset

Method	Accuracy (%)
<b>UMAP-3-CNN</b>	<b>98.80</b>
T-SNE-CNN <sup>2</sup>	97.89
PCA-CNN	96.79
DC-CNN <sup>3</sup>	95.50
DR-CNN <sup>4</sup>	94.93
Multiscale-CNN	87.42
1D-CNN <sup>5</sup>	66.36
SVM <sup>6</sup>	74.81
RF-200 <sup>7</sup>	61.89

- UMAP-CNN achieves the best overall accuracy.

---

<sup>2</sup>Gao et al. 2020.

<sup>3</sup>Zhang et al. 2017.

<sup>4</sup>Gao et al. 2020.

<sup>5</sup>Chen et al. 2016.

<sup>6</sup>Mercier and Lennon 2003.

<sup>7</sup>Joelsson, Benediktsson, and Sveinsson 2005.

- **UMAP Advantages:**

- Preserves topological data structures.
- Non-linear dependencies in XRT HSI are effectively represented.
- Outperforms PCA/NMF in segmentation, regression, and classification.
- Dimensionality reduction enhances robustness by removing redundancy.







- **Conclusion:**

- UMAP-based dimensionality reduction improves all evaluated tasks.
- Demonstrates strong potential for XRT hyperspectral imaging.

# Thank you!

Questions?

# References

-  Chen, Yushi et al. (2016). “Deep feature extraction and classification of hyperspectral images based on convolutional neural networks”. In: *IEEE transactions on geoscience and remote sensing* 54.10, pp. 6232–6251.
-  Gao, Lianru et al. (2020). “Combining t-Distributed Stochastic Neighbor Embedding With Convolutional Neural Networks for Hyperspectral Image Classification”. In: *IEEE Geoscience and Remote Sensing Letters* 17.8, pp. 1368–1372. DOI: 10.1109/LGRS.2019.2945122.
-  Joelsson, Sveinn R, Jon Atli Benediktsson, and Johannes R Sveinsson (2005). “Random forest classifiers for hyperspectral data”. In: *Proceedings. 2005 IEEE International Geoscience and Remote Sensing Symposium, 2005. IGARSS'05*. Vol. 1. IEEE, 4–pp.
-  McInnes, Leland, John Healy, and James Melville (Sept. 2020). *UMAP: Uniform Manifold Approximation and Projection for Dimension Reduction*. arXiv:1802.03426 [cs, stat]. DOI: 10.48550/arXiv.1802.03426. URL: <http://arxiv.org/abs/1802.03426> (visited on 10/27/2023).
-  Mercier, Grégoire and Marc Lennon (2003). “Support vector machines for hyperspectral image classification with spectral-based kernels”. In: 

# Evaluation Metrics

## Intersection over Union (IoU)

$$\text{IoU} = \frac{|P \cap G|}{|P \cup G|}$$

Measures the overlap between predicted ( $P$ ) and ground-truth ( $G$ ) segmentation masks.

## Dice Coefficient

$$\text{Dice} = \frac{2|P \cap G|}{|P| + |G|}$$

A harmonic mean of precision and recall, emphasizing overlap quality.

## Mutual Information (MI)

$$\text{MI}(X, Y) = \sum_{x \in X} \sum_{y \in Y} p(x, y) \log \frac{p(x, y)}{p(x)p(y)}$$

Quantifies the amount of shared information between two random variables